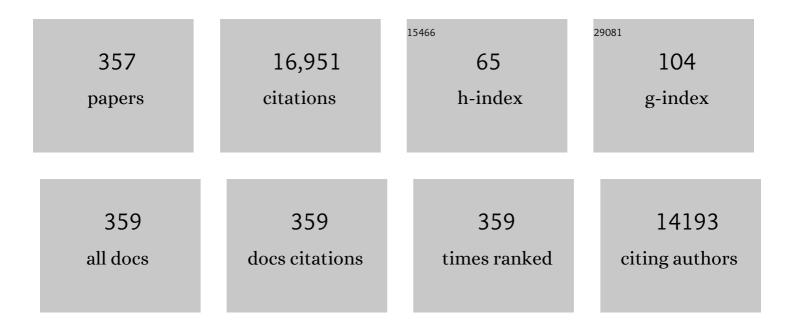
## Hyoun-Ee Kim

List of Publications by Year in descending order

Source: https://exaly.com/author-pdf/1697097/publications.pdf Version: 2024-02-01



HVOUN-FE KIM

#	Article	IF	CITATIONS
1	Improved biological performance of Ti implants due to surface modification by micro-arc oxidation. Biomaterials, 2004, 25, 2867-2875.	5.7	629
2	Magnetoelectric Effect in Composites of Magnetostrictive and Piezoelectric Materials. , 2002, 8, 107-119.		628
3	Hydroxyapatite/poly(ε-caprolactone) composite coatings on hydroxyapatite porous bone scaffold for drug delivery. Biomaterials, 2004, 25, 1279-1287.	5.7	480
4	Stimulation of osteoblast responses to biomimetic nanocomposites of gelatin–hydroxyapatite for tissue engineering scaffolds. Biomaterials, 2005, 26, 5221-5230.	5.7	416
5	Hydroxyapatite coating on titanium substrate with titania buffer layer processed by sol–gel method. Biomaterials, 2004, 25, 2533-2538.	5.7	360
6	Title is missing!. , 2001, 7, 17-24.		300
7	Effect of the Magnetostrictive Layer on Magnetoelectric Properties in Lead Zirconate Titanate/Terfenolâ€Ð Laminate Composites. Journal of the American Ceramic Society, 2001, 84, 2905-2908.	1.9	265
8	The electron beam deposition of titanium on polyetheretherketone (PEEK) and the resulting enhanced biological properties. Biomaterials, 2010, 31, 3465-3470.	5.7	230
9	Membrane of hybrid chitosan–silica xerogel for guided bone regeneration. Biomaterials, 2009, 30, 743-750.	5.7	228
10	Fluor-hydroxyapatite sol–gel coating on titanium substrate for hard tissue implants. Biomaterials, 2004, 25, 3351-3358.	5.7	212
11	Aligned porous alumina ceramics with high compressive strengths for bone tissue engineering. Scripta Materialia, 2008, 58, 537-540.	2.6	181
12	Porous ZrO2 bone scaffold coated with hydroxyapatite with fluorapatite intermediate layer. Biomaterials, 2003, 24, 3277-3284.	5.7	178
13	Hydroxyapatite porous scaffold engineered with biological polymer hybrid coating for antibiotic Vancomycin release. Journal of Materials Science: Materials in Medicine, 2005, 16, 189-195.	1.7	176
14	Hydroxyapatite and gelatin composite foams processed via novel freeze-drying and crosslinking for use as temporary hard tissue scaffolds. Journal of Biomedical Materials Research - Part A, 2005, 72A, 136-145.	2.1	167
15	Perovskite stabilization and electromechanical properties of polycrystalline lead zinc niobate–lead zirconate titanate. Journal of Applied Physics, 2002, 91, 317.	1.1	157
16	<i>In vitro</i> / <i>in vivo</i> biocompatibility and mechanical properties of bioactive glass nanofiber and poly(εâ€caprolactone) composite materials. Journal of Biomedical Materials Research - Part B Applied Biomaterials, 2009, 91B, 213-220.	1.6	151
17	Densification and Mechanical Properties of B <sub>4</sub> C with Al <sub>2</sub> O <sub>3</sub> as a Sintering Aid. Journal of the American Ceramic Society, 2000, 83, 2863-2865.	1.9	149
18	Mechanical and in vitro biological performances of hydroxyapatite–carbon nanotube composite coatings deposited on Ti by aerosol deposition. Acta Biomaterialia, 2009, 5, 3205-3214.	4.1	148

#	Article	IF	CITATIONS
19	Highly Aligned Porous Silicon Carbide Ceramics by Freezing Polycarbosilane/Camphene Solution. Journal of the American Ceramic Society, 2007, 90, 1753-1759.	1.9	142
20	Porous scaffolds of gelatin-hydroxyapatite nanocomposites obtained by biomimetic approach: Characterization and antibiotic drug release. Journal of Biomedical Materials Research - Part B Applied Biomaterials, 2005, 74B, 686-698.	1.6	141
21	Microstructural Evolution and Mechanical Properties of Si <sub>3</sub> N <sub>4</sub> with Yb <sub>2</sub> O <sub>3</sub> as a Sintering Additive. Journal of the American Ceramic Society, 1997, 80, 750-756.	1.9	136
22	Formation of hydroxyapatite within porous TiO2 layer by micro-arc oxidation coupled with electrophoretic deposition. Acta Biomaterialia, 2009, 5, 2196-2205.	4.1	130
23	Improvement in biocompatibility of ZrO2–Al2O3 nano-composite by addition of HA. Biomaterials, 2005, 26, 509-517.	5.7	128
24	Bioactive glass nanofiber–collagen nanocomposite as a novel bone regeneration matrix. Journal of Biomedical Materials Research - Part A, 2006, 79A, 698-705.	2.1	123
25	Highly porous hydroxyapatite bioceramics with interconnected pore channels using camphene-based freeze casting. Materials Letters, 2007, 61, 2270-2273.	1.3	123
26	Sol–gel derived fluor-hydroxyapatite biocoatings on zirconia substrate. Biomaterials, 2004, 25, 2919-2926.	5.7	122
27	Biocompatibility of titanium implants modified by microarc oxidation and hydroxyapatite coating. Journal of Biomedical Materials Research - Part A, 2005, 73A, 48-54.	2.1	122
28	Enhancement of bio-stability and mechanical properties of hyaluronic acid hydrogels by tannic acid treatment. Carbohydrate Polymers, 2018, 186, 290-298.	5.1	115
29	Reinforcement of Hydroxyapatite Bioceramic by Addition of ZrO2 Coated with Al2O3. Journal of the American Ceramic Society, 1999, 82, 2963-2968.	1.9	113
30	Generation of Large Pore Channels for Bone Tissue Engineering Using Camphene-Based Freeze Casting. Journal of the American Ceramic Society, 2007, 90, 1744-1752.	1.9	113
31	Effect of CaF2 on densification and properties of hydroxyapatite–zirconia composites for biomedical applications. Biomaterials, 2002, 23, 4113-4121.	5.7	109
32	Nanostructured poly(ε-caprolactone)–silica xerogel fibrous membrane for guided bone regeneration. Acta Biomaterialia, 2010, 6, 3557-3565.	4.1	109
33	Chitosan/nanohydroxyapatite composite membranes via dynamic filtration for guided bone regeneration. Journal of Biomedical Materials Research - Part A, 2009, 88A, 569-580.	2.1	108
34	Development of hydroxyapatite bone scaffold for controlled drug release via poly(?-caprolactone) and hydroxyapatite hybrid coatings. Journal of Biomedical Materials Research Part B, 2004, 70B, 240-249.	3.0	105
35	Effect of Polystyrene Addition on Freeze Casting of Ceramic/Camphene Slurry for Ultra-High Porosity Ceramics with Aligned Pore Channels. Journal of the American Ceramic Society, 2006, 89, 3646-3653.	1.9	104
36	Nanofibrous gelatin–silica hybrid scaffolds mimicking the native extracellular matrix (ECM) using thermally induced phase separation. Journal of Materials Chemistry, 2012, 22, 14133.	6.7	104

#	Article	IF	CITATIONS
37	Oxidation Behavior of Titanium Boride at Elevated Temperatures. Journal of the American Ceramic Society, 2001, 84, 239-241.	1.9	103
38	Strong and biocompatible poly(lactic acid) membrane enhanced by Ti3C2Tz (MXene) nanosheets for Guided bone regeneration. Materials Letters, 2018, 229, 114-117.	1.3	100
39	Hydroxyapatiteâ€coated magnesium implants with improved <i>in vitro</i> and <i>in vivo</i> biocorrosion, biocompatibility, and bone response. Journal of Biomedical Materials Research - Part A, 2014, 102, 429-441.	2.1	97
40	Calcium Phosphate Bioceramics with Various Porosities and Dissolution Rates. Journal of the American Ceramic Society, 2002, 85, 3129-3131.	1.9	96
41	Densification and Mechanical Properties of Titanium Diboride with Silicon Nitride as a Sintering Aid. Journal of the American Ceramic Society, 1999, 82, 3037-3042.	1.9	96
42	Freezing Dilute Ceramic/Camphene Slurry for Ultra-High Porosity Ceramics with Completely Interconnected Pore Networks. Journal of the American Ceramic Society, 2006, 89, 3089-3093.	1.9	95
43	Reinforcement of Hydroxyapatite Bioceramic by Addition of Ni <sub>3</sub> Al and Al <sub>2</sub> O <sub>3</sub> . Journal of the American Ceramic Society, 1998, 81, 1743-1748.	1.9	92
44	Osteoconductive hydroxyapatite coated PEEK for spinal fusion surgery. Applied Surface Science, 2013, 283, 6-11.	3.1	92
45	Strontium substituted calcium phosphate biphasic ceramics obtained by a powder precipitation method. Journal of Materials Science: Materials in Medicine, 2004, 15, 1129-1134.	1.7	89
46	Calcium phosphates and glass composite coatings on zirconia for enhanced biocompatibility. Biomaterials, 2004, 25, 4203-4213.	5.7	89
47	Fabrication of strong, bioactive vascular grafts with PCL/collagen and PCL/silica bilayers for small-diameter vascular applications. Materials and Design, 2019, 181, 108079.	3.3	89
48	Fluoridated apatite coatings on titanium obtained by electron-beam deposition. Biomaterials, 2005, 26, 3843-3851.	5.7	87
49	Fabrication of Porous PZT?PZN Piezoelectric Ceramics With High Hydrostatic Figure of Merits Using Camphene-Based Freeze Casting. Journal of the American Ceramic Society, 2007, 90, 2807-2813.	1.9	86
50	Reverse freeze casting: A new method for fabricating highly porous titanium scaffolds with aligned large pores. Acta Biomaterialia, 2012, 8, 2401-2410.	4.1	86
51	Electrospun fibrous web of collagen–apatite precipitated nanocomposite for bone regeneration. Journal of Materials Science: Materials in Medicine, 2008, 19, 2925-2932.	1.7	85
52	Collagen/hydroxyapatite composite nanofibers by electrospinning. Materials Letters, 2008, 62, 3055-3058.	1.3	85
53	Hydroxyapatite and titania sol-gel composite coatings on titanium for hard tissue implants; Mechanical andin vitro biological performance. Journal of Biomedical Materials Research Part B, 2005, 72B, 1-8.	3.0	84
54	Threeâ€layered membranes of collagen/hydroxyapatite and chitosan for guided bone regeneration. Journal of Biomedical Materials Research - Part B Applied Biomaterials, 2008, 87B, 132-138.	1.6	83

#	Article	IF	CITATIONS
55	A bioactive coating of a silica xerogel/chitosan hybrid on titanium by a room temperature sol–gel process. Acta Biomaterialia, 2010, 6, 302-307.	4.1	83
56	Hydroxyapatite-TiO2 Hybrid Coating on Ti Implants. Journal of Biomaterials Applications, 2006, 20, 195-208.	1.2	82
57	Hydroxyapatite coating on magnesium with MgF2 interlayer for enhanced corrosion resistance and biocompatibility. Journal of Materials Science: Materials in Medicine, 2011, 22, 2437-2447.	1.7	82
58	Stability and cellular responses to fluorapatite–collagen composites. Biomaterials, 2005, 26, 2957-2963.	5.7	81
59	Improved compressive strength of reticulated porous zirconia using carbon coated polymeric sponge as novel template. Materials Letters, 2006, 60, 2507-2510.	1.3	79
60	Dynamic freeze casting for the production of porous titanium (Ti) scaffolds. Materials Science and Engineering C, 2013, 33, 59-63.	3.8	78
61	Collagen-apatite nanocomposite membranes for guided bone regeneration. Journal of Biomedical Materials Research - Part B Applied Biomaterials, 2007, 83B, 248-257.	1.6	77
62	Effect of Heating Rate on the Sintering Behavior and the Piezoelectric Properties of Lead Zirconate Titanate Ceramics. Journal of the American Ceramic Society, 2001, 84, 902-904.	1.9	76
63	Bone morphogenic protein-2 (BMP-2) loaded hybrid coating on porous hydroxyapatite scaffolds for bone tissue engineering. Journal of Materials Science: Materials in Medicine, 2013, 24, 773-782.	1.7	76
64	Cytocompatibility of Ti <sub>3</sub> AlC <sub>2</sub> , Ti <sub>3</sub> SiC <sub>2</sub> , and Ti <sub>2</sub> AlN: <i>In Vitro</i> Tests and First-Principles Calculations. ACS Biomaterials Science and Engineering, 2017, 3, 2293-2301.	2.6	75
65	Porous titanium (Ti) scaffolds by freezing TiH2/camphene slurries. Materials Letters, 2008, 62, 4506-4508.	1.3	72
66	Calcium Sulfate Hemihydrate Powders with a Controlled Morphology for Use as Bone Cement. Journal of the American Ceramic Society, 2008, 91, 2039-2042.	1.9	71
67	Fabrication of porous titanium scaffold with controlled porous structure and net-shape using magnesium as spacer. Materials Science and Engineering C, 2013, 33, 2808-2815.	3.8	70
68	Biomimetic porous Mg with tunable mechanical properties and biodegradation rates for bone regeneration. Acta Biomaterialia, 2019, 84, 453-467.	4.1	69
69	Effect of Lead Content on the Structure and Electrical Properties of Pb((Zn <sub>1/3</sub> Nb <sub>2/3</sub> ) <sub>0.5</sub> (Zr <sub>0.47</sub> Ti <sub>0.53</sub> ) <sub>0.5<td>/su<b>b</b><i>x</i>)O<s< td=""><td>subø3</td></s<></td></sub>	/su <b>b</b> <i>x</i> )O <s< td=""><td>subø3</td></s<>	subø3
70	Pressureless Sintering and Mechanical and Biological Properties of Fluorâ€hydroxyapatite Composites with Zirconia. Journal of the American Ceramic Society, 2003, 86, 2019-2026.	1.9	67
71	Bioactive nanocomposite coatings of collagen/hydroxyapatite on titanium substrates. Journal of Materials Science: Materials in Medicine, 2008, 19, 2453-2461.	1.7	67
72	Low-temperature sintering of MnO2-doped PZT–PZN Piezoelectric ceramics. Journal of Electroceramics, 2007, 18, 311-315.	0.8	64

#	Article	IF	CITATIONS
73	Production of Poly(ε-Caprolactone)/Hydroxyapatite Composite Scaffolds with a Tailored Macro/Micro-Porous Structure, High Mechanical Properties, and Excellent Bioactivity. Materials, 2017, 10, 1123.	1.3	64
74	Biological performance of calcium phosphate films formed on commercially pure Ti by electron-beam evaporation. Biomaterials, 2002, 23, 609-615.	5.7	63
75	Fabrication of porous titanium scaffolds with high compressive strength using camphene-based freeze casting. Materials Letters, 2009, 63, 1502-1504.	1.3	63
76	Photocurable ceramic slurry using solid camphor as novel diluent for conventional digital light processing (DLP) process. Journal of the European Ceramic Society, 2019, 39, 4358-4365.	2.8	63
77	Measurement of piezoelectric coefficients of lead zirconate titanate thin films by strain-monitoring pneumatic loading method. Applied Physics Letters, 2002, 80, 4606-4608.	1.5	62
78	Fibrillar assembly and stability of collagen coating on titanium for improved osteoblast responses. Journal of Biomedical Materials Research - Part A, 2005, 75A, 629-638.	2.1	61
79	Fabrication of titanium scaffolds with porosity and pore size gradients by sequential freeze casting. Materials Letters, 2009, 63, 1545-1547.	1.3	61
80	Highly porous hydroxyapatite scaffolds with elongated pores using stretched polymeric sponges as novel template. Materials Letters, 2009, 63, 1702-1704.	1.3	61
81	Strong and Biostable Hyaluronic Acid–Calcium Phosphate Nanocomposite Hydrogel via in Situ Precipitation Process. Biomacromolecules, 2016, 17, 841-851.	2.6	60
82	Effect of biphasic calcium phosphates on drug release and biological and mechanical properties of poly(?-caprolactone) composite membranes. Journal of Biomedical Materials Research Part B, 2004, 70A, 467-479.	3.0	59
83	Effect of Flaw State on the Strength of Brittle Coatings on Soft Substrates. Journal of the American Ceramic Society, 2001, 84, 2377-2384.	1.9	58
84	Piezoelectric Properties of PZTâ€Based Ceramic with Highly Aligned Pores. Journal of the American Ceramic Society, 2008, 91, 1912-1915.	1.9	58
85	Fabrication and compressive strength of porous hydroxyapatite scaffolds with a functionally graded core/shell structure. Journal of the European Ceramic Society, 2011, 31, 13-18.	2.8	58
86	Hierarchical micro-nano structured Ti6Al4V surface topography via two-step etching process for enhanced hydrophilicity and osteoblastic responses. Materials Science and Engineering C, 2017, 73, 90-98.	3.8	57
87	Dense Nanostructured Hydroxyapatite Coating on Titanium by Aerosol Deposition. Journal of the American Ceramic Society, 2009, 92, 683-687.	1.9	56
88	Blend fibers of chitosan–agarose by electrospinning. Materials Letters, 2009, 63, 2510-2512.	1.3	56
89	Compressive strength and processing of camphene-based freeze cast calcium phosphate scaffolds with aligned pores. Materials Letters, 2009, 63, 1548-1550.	1.3	55
90	Aerosol deposition of silicon-substituted hydroxyapatite coatings for biomedical applications. Thin Solid Films, 2010, 518, 2194-2199.	0.8	55

#	Article	IF	CITATIONS
91	Effect of Hotâ€Pressing Temperature on Densification and Mechanical Properties of Titanium Diboride with Silicon Nitride as a Sintering Aid. Journal of the American Ceramic Society, 2000, 83, 1542-1544.	1.9	54
92	Porous Hydroxyapatite Scaffolds Coated With Bioactive Apatite–Wollastonite Glass–Ceramics. Journal of the American Ceramic Society, 2007, 90, 2703-2708.	1.9	52
93	Electro-optic characteristics of (001)-oriented Ba0.6Sr0.4TiO3 thin films. Applied Physics Letters, 2003, 82, 1455-1457.	1.5	51
94	Lowâ€Temperature Sintering and Piezoelectric Properties of 0.6Pb(Zr <sub>0.47</sub> Ti <sub>0.5</sub> 3)O <sub>3</sub> ·0.4Pb(Zn <sub>1/3</sub> Nb <sub>2/</sub> 3)C Ceramics. Journal of the American Ceramic Society, 2004, 87, 1238-1243.	) <s∎bos>3<!--</td--><td>/subs</td></s∎bos>	/subs
95	Oxidation and Strength Retention of Monolithic Si <sub>3</sub> N <sub>4</sub> and Nanocomposite Si <sub>3</sub> N <sub>4</sub> â€5iC with Yb <sub>2</sub> O <sub>3</sub> as a Sintering Aid. Journal of the American Ceramic Society, 1998, 81, 2130-2134.	1.9	51
96	Sol-gel-modified titanium with hydroxyapatite thin films and effect on osteoblast-like cell responses. Journal of Biomedical Materials Research - Part A, 2005, 74A, 294-305.	2.1	51
97	Highly porous titanium (Ti) scaffolds with bioactive microporous hydroxyapatite/TiO2 hybrid coating layer. Materials Letters, 2009, 63, 1995-1998.	1.3	51
98	Novel strategy for mechanically tunable and bioactive metal implants. Biomaterials, 2015, 37, 49-61.	5.7	51
99	Hydroxyapatite and fluor-hydroxyapatite layered film on titanium processed by a sol-gel route for hard-tissue implants. Journal of Biomedical Materials Research Part B, 2004, 71B, 66-76.	3.0	50
100	Fabrication of a Porous Bioactive Glass–Ceramic Using Room-Temperature Freeze Casting. Journal of the American Ceramic Society, 2006, 89, 2649-2653.	1.9	50
101	Silica xerogel-chitosan nano-hybrids for use as drug eluting bone replacement. Journal of Materials Science: Materials in Medicine, 2010, 21, 207-214.	1.7	49
102	Production and bio-corrosion resistance of porous magnesium with hydroxyapatite coating for biomedical applications. Materials Letters, 2013, 108, 122-124.	1.3	49
103	Piezoelectric and ferroelectric properties of 1-î¼m-thick lead zirconate titanate film fabricated by a double-spin-coating process. Applied Physics Letters, 2004, 85, 2322-2324.	1.5	48
104	Porous alumina ceramic scaffolds with biomimetic macro/micro-porous structure using three-dimensional (3-D) ceramic/camphene-based extrusion. Ceramics International, 2015, 41, 12371-12377.	2.3	48
105	Construction of tantalum/poly(ether imide) coatings on magnesium implants with both corrosion protection and osseointegration properties. Bioactive Materials, 2021, 6, 1189-1200.	8.6	48
106	Effect of calcinations of starting powder on mechanical properties of hydroxyapatite-alumina bioceramic composite. Journal of Materials Science: Materials in Medicine, 2002, 13, 307-310.	1.7	47
107	Functionally gradient chitosan/hydroxyapatite composite scaffolds for controlled drug release. Journal of Biomedical Materials Research - Part B Applied Biomaterials, 2009, 90B, 275-282.	1.6	47
108	Enhanced performance of fluorine substituted hydroxyapatite composites for hard tissue engineering. Journal of Materials Science: Materials in Medicine, 2003, 14, 899-904.	1.7	46

#	Article	IF	CITATIONS
109	Effect of lead zinc niobate addition on sintering behavior and piezoelectric properties of lead zirconate titanate ceramic. Journal of Materials Research, 2004, 19, 2553-2556.	1.2	46
110	Dissolution control and cellular responses of calcium phosphate coatings on zirconia porous scaffold. Journal of Biomedical Materials Research Part B, 2004, 68A, 522-530.	3.0	46
111	Bone Formation on the Apatite-coated Zirconia Porous Scaffolds within a Rabbit Calvarial Defect. Journal of Biomaterials Applications, 2008, 22, 485-504.	1.2	46
112	Creation of nanoporous TiO <sub>2</sub> surface onto polyetheretherketone for effective immobilization and delivery of bone morphogenetic protein. Journal of Biomedical Materials Research - Part A, 2014, 102, 793-800.	2.1	45
113	Fabrication of Macrochannelled-Hydroxyapatite Bioceramic by a Coextrusion Process. Journal of the American Ceramic Society, 2002, 85, 2578-2580.	1.9	44
114	In situ Fabrication of a Dense/Porous Bi-layered Ceramic Composite using Freeze Casting of a Ceramic-Camphene Slurry. Journal of the American Ceramic Society, 2006, 89, 763-766.	1.9	44
115	Sol–gel derived nanoscale bioactive glass (NBC) particles reinforced poly(ε-caprolactone) composites for bone tissue engineering. Materials Science and Engineering C, 2013, 33, 1102-1108.	3.8	44
116	Fabrication of poly(lactic acid)/Ti composite scaffolds with enhanced mechanical properties and biocompatibility via fused filament fabrication (FFF)–based 3D printing. Additive Manufacturing, 2019, 30, 100883.	1.7	44
117	Microstructural Evolution of Transparent PLZT Ceramics Sintered in Air and Oxygen Atmospheres. Journal of the American Ceramic Society, 2001, 84, 1465-1469.	1.9	43
118	Fabrication of a Highly Porous Bioactive Glass-Ceramic Scaffold with a High Surface Area and Strength. Journal of the American Ceramic Society, 2006, 89, 391-394.	1.9	43
119	Highly aligned porous Ti scaffold coated with bone morphogenetic proteinâ€loaded silica/chitosan hybrid for enhanced bone regeneration. Journal of Biomedical Materials Research - Part B Applied Biomaterials, 2014, 102, 913-921.	1.6	43
120	MgF2-coated porous magnesium/alumina scaffolds with improved strength, corrosion resistance, and biological performance for biomedical applications. Materials Science and Engineering C, 2016, 62, 634-642.	3.8	43
121	Enhanced Osseointegration Ability of Poly(lactic acid) via Tantalum Sputtering-Based Plasma Immersion Ion Implantation. ACS Applied Materials & Interfaces, 2019, 11, 10492-10504.	4.0	43
122	Biodegradable magnesium alloy (WE43) in boneâ€fixation plate and screw. Journal of Biomedical Materials Research - Part B Applied Biomaterials, 2020, 108, 2505-2512.	1.6	43
123	Reaction sintering and mechanical properties of B <sub>4</sub> C with addition of ZrO <sub>2</sub> . Journal of Materials Research, 2000, 15, 2431-2436.	1.2	42
124	Enhancing biocompatibility and corrosion resistance of Mg implants via surface treatments. Journal of Biomaterials Applications, 2012, 27, 469-476.	1.2	42
125	Bioactive glass microspheres as reinforcement for improving the mechanical properties and biological performance of poly(ε aprolactone) polymer for bone tissue regeneration. Journal of Biomedical Materials Research - Part B Applied Biomaterials, 2012, 100B, 967-975.	1.6	42
126	<i>In Situ</i> Synthesis of Porous Silicon Carbide (SiC) Ceramics Decorated with SiC Nanowires. Journal of the American Ceramic Society, 2007, 90, 3759-3766.	1.9	41

#	Article	IF	CITATIONS
127	Macroporous alumina scaffolds consisting of highly microporous hollow filaments using three-dimensional ceramic/camphene-based co-extrusion. Journal of the European Ceramic Society, 2015, 35, 4623-4627.	2.8	41
128	The Production of Porous Hydroxyapatite Scaffolds with Graded Porosity by Sequential Freeze-Casting. Materials, 2017, 10, 367.	1.3	41
129	Oxidation Behavior and Flexural Strength of Aluminum Nitride Exposed to Air at Elevated Temperatures. Journal of the American Ceramic Society, 1994, 77, 1037-1041.	1.9	40
130	Formation and characterization of hydroxyapatite coating layer on Ti-based metal implant by electron-beam deposition. Journal of Materials Research, 1999, 14, 2980-2985.	1.2	40
131	Effect of lanthanum on the piezoelectric properties of lead zirconate titanate–lead zinc niobate ceramics. Journal of Materials Research, 2003, 18, 1765-1770.	1.2	40
132	Porous Calcium Phosphate Ceramic Scaffolds with Tailored Pore Orientations and Mechanical Properties Using Lithography-Based Ceramic 3D Printing Technique. Materials, 2018, 11, 1711.	1.3	40
133	Preparation and Improvement in the Electrical Properties of Lead-zinc-niobate–based Ceramics by Thermal Treatments. Journal of Materials Research, 2002, 17, 180-185.	1.2	39
134	Hydroxyapatite (HA)/poly-l-lactic acid (PLLA) dual coating on magnesium alloy under deformation for biomedical applications. Journal of Materials Science: Materials in Medicine, 2016, 27, 34.	1.7	39
135	Reaction Sintering and Mechanical Properties of Hydroxyapatite–Zirconia Composites with Calcium Fluoride Additions. Journal of the American Ceramic Society, 2002, 85, 1634-1636.	1.9	38
136	Microsphere of apatite-gelatin nanocomposite as bone regenerative filler. Journal of Materials Science: Materials in Medicine, 2005, 16, 1105-1109.	1.7	37
137	Effects of Residual Stress on the Electrical Properties of PZT Films. Journal of the American Ceramic Society, 2007, 90, 1077-1080.	1.9	37
138	Effect of the HA/βâ€TCP Ratio on the Biological Performance of Calcium Phosphate Ceramic Coatings Fabricated by a Roomâ€Temperature Powder Spray in Vacuum. Journal of the American Ceramic Society, 2009, 92, 793-799.	1.9	37
139	Design and characterization of broadband magnetoelectric sensor. Journal of Applied Physics, 2009, 105, .	1.1	37
140	Polyurethane-silica hybrid foams from a one-step foaming reaction, coupled with a sol-gel process, for enhanced wound healing. Materials Science and Engineering C, 2017, 79, 866-874.	3.8	37
141	Sol–Gel Preparation and Properties of Fluoride‣ubstituted Hydroxyapatite Powders. Journal of the American Ceramic Society, 2004, 87, 1939-1944.	1.9	36
142	Hydroxyapatite (HA) bone scaffolds with controlled macrochannel pores. Journal of Materials Science: Materials in Medicine, 2006, 17, 517-521.	1.7	36
143	Utility of tantalum (Ta) coating to improve surface hardness in vitro bioactivity and biocompatibility of Co–Cr. Thin Solid Films, 2013, 536, 269-274.	0.8	36
144	Accelerated bony defect healing by chitosan/silica hybrid membrane with localized bone morphogenetic protein-2 delivery. Materials Science and Engineering C, 2016, 59, 339-345.	3.8	36

#	Article	IF	CITATIONS
145	High-Temperature Gaseous Corrosion of Si3N4 in H2-H2O and Ar-O2 Environments. Journal of the American Ceramic Society, 1990, 73, 3007-3014.	1.9	35
146	Hard-tissue-engineered zirconia porous scaffolds with hydroxyapatite sol-gel and slurry coatings. Journal of Biomedical Materials Research Part B, 2004, 70B, 270-277.	3.0	35
147	Fabrication of poly(ε-caprolactone)/hydroxyapatite scaffold using rapid direct deposition. Materials Letters, 2006, 60, 1184-1187.	1.3	35
148	Creation of hierarchical micro/nano-porous TiO2 surface layer onto Ti implants for improved biocompatibility. Surface and Coatings Technology, 2014, 251, 226-231.	2.2	35
149	Polydeoxyribonucleotide-delivering therapeutic hydrogel for diabetic wound healing. Scientific Reports, 2020, 10, 16811.	1.6	35
150	Properties of fluoridated hydroxyapatite–alumina biological composites densified with addition of CaF2. Materials Science and Engineering C, 2003, 23, 515-521.	3.8	34
151	Tantalum-coated polylactic acid fibrous membranes for guided bone regeneration. Materials Science and Engineering C, 2020, 115, 111112.	3.8	34
152	Effect of annealing atmosphere on domain structures and electromechanical properties of Pb(Zn1/3Nb2/3)O3-based ceramics. Applied Physics Letters, 2001, 79, 1658-1660.	1.5	33
153	Production of highly porous triphasic calcium phosphate scaffolds with excellent in vitro bioactivity using vacuum-assisted foaming of ceramic suspension (VFC) technique. Ceramics International, 2013, 39, 5879-5885.	2.3	33
154	Effective Wound Healing by Antibacterial and Bioactive Calcium-Fluoride-Containing Composite Hydrogel Dressings Prepared Using in Situ Precipitation. ACS Biomaterials Science and Engineering, 2018, 4, 2380-2389.	2.6	33
155	Reduced fibrous capsule formation at nano-engineered silicone surfaces via tantalum ion implantation. Biomaterials Science, 2019, 7, 2907-2919.	2.6	33
156	Studies on calcium phosphate coatings. Surface and Coatings Technology, 2000, 131, 181-186.	2.2	32
157	Coâ€firing of PZNâ€PZT Flextensional Actuators. Journal of the American Ceramic Society, 2004, 87, 1663-1668.	1.9	32
158	Porous calcium phosphate–collagen composite microspheres for effective growth factor delivery and bone tissue regeneration. Materials Science and Engineering C, 2020, 109, 110480.	3.8	32
159	In-situ fabrication of porous hydroxyapatite (HA) scaffolds with dense shells by freezing HA/camphene slurry. Materials Letters, 2008, 62, 1700-1703.	1.3	31
160	Poly(ether imide)-silica hybrid coatings for tunable corrosion behavior and improved biocompatibility of magnesium implants. Biomedical Materials (Bristol), 2016, 11, 035003.	1.7	31
161	Calcium Phosphate–Collagen Scaffold with Aligned Pore Channels for Enhanced Osteochondral Regeneration. Advanced Healthcare Materials, 2017, 6, 1700966.	3.9	31
162	Effect of Hydrogen-Water Atmospheres on Corrosion and Flexural Strength of Sintered alpha-Silicon Carbide. Journal of the American Ceramic Society, 1990, 73, 694-699.	1.9	30

#	Article	IF	CITATIONS
163	Fibrous membrane of nanoâ€hybrid polyâ€ <scp>L</scp> â€lactic acid/silica xerogel for guided bone regeneration. Journal of Biomedical Materials Research - Part B Applied Biomaterials, 2012, 100B, 321-330.	1.6	30
164	Innovative micro-textured hydroxyapatite and poly(I-lactic)-acid polymer composite film as a flexible, corrosion resistant, biocompatible, and bioactive coating for Mg implants. Materials Science and Engineering C, 2017, 81, 97-103.	3.8	30
165	Hyaluronic Acid-Based Hybrid Hydrogel Microspheres with Enhanced Structural Stability and High Injectability. ACS Omega, 2019, 4, 13834-13844.	1.6	30
166	One-pot synthesis of silane-modified hyaluronic acid hydrogels for effective antibacterial drug delivery via sol–gel stabilization. Colloids and Surfaces B: Biointerfaces, 2019, 174, 308-315.	2.5	30
167	Orientation Control of Lead Zirconate Titanate Film by Combination of Sol-Gel and Sputtering Deposition. Journal of Materials Research, 2005, 20, 243-246.	1.2	29
168	Mechanical performance and osteoblast-like cell responses of fluorine-substituted hydroxyapatite and zirconia dense composite. Journal of Biomedical Materials Research - Part A, 2005, 72A, 258-268.	2.1	29
169	Nano-Sized Hydroxyapatite Coatings on Ti Substrate with TiO2Buffer Layer by E-beam Deposition. Journal of the American Ceramic Society, 2007, 90, 50-56.	1.9	29
170	Threeâ€dimensional Ceramic/Campheneâ€based Coextrusion for Unidirectionally Macrochanneled Alumina Ceramics with Controlled Porous Walls. Journal of the American Ceramic Society, 2014, 97, 32-34.	1.9	29
171	Reinforcement of polyetheretherketone polymer with titanium for improved mechanical properties and <i>in vitro</i> biocompatibility. Journal of Biomedical Materials Research - Part B Applied Biomaterials, 2016, 104, 141-148.	1.6	29
172	Macroporous Alumina Ceramics with Aligned Microporous Walls by Unidirectionally Freezing Foamed Aqueous Ceramic Suspensions. Journal of the American Ceramic Society, 2010, 93, 1580-1582.	1.9	28
173	Synthesis and Bioactivity of Sol–Gel Derived Porous, Bioactive Glass Microspheres Using Chitosan as Novel Biomolecular Template. Journal of the American Ceramic Society, 2012, 95, 30-33.	1.9	28
174	Porous alumina ceramics with highly aligned pores by heat-treating extruded alumina/camphene body at temperature near its solidification point. Journal of the European Ceramic Society, 2012, 32, 1029-1034.	2.8	28
175	Use of a poly(ether imide) coating to improve corrosion resistance and biocompatibility of magnesium (Mg) implant for orthopedic applications. Journal of Biomedical Materials Research - Part A, 2013, 101A, 1708-1715.	2.1	28
176	Hydroxyapatite Microspheres as an Additive to Enhance Radiopacity, Biocompatibility, and Osteoconductivity of Poly(methyl methacrylate) Bone Cement. Materials, 2018, 11, 258.	1.3	28
177	Composition and Crystallization of Hydroxyapatite Coating Layer Formed by Electron Beam Deposition. Journal of the American Ceramic Society, 2003, 86, 186-188.	1.9	27
178	Improvement of Hydroxyapatite Sol–Gel Coating on Titanium with Ammonium Hydroxide Addition. Journal of the American Ceramic Society, 2005, 88, 154-159.	1.9	27
179	Effect of fluorine addition on the biological performance of hydroxyapatite coatings on Ti by aerosol deposition. Journal of Biomaterials Applications, 2013, 27, 587-594.	1.2	27
180	Multi-scale porous Ti6Al4V scaffolds with enhanced strength and biocompatibility formed via dynamic freeze-casting coupled with micro-arc oxidation. Materials Letters, 2016, 185, 21-24.	1.3	27

#	Article	IF	CITATIONS
181	Multiscale porous titanium surfaces via a two-step etching process for improved mechanical and biological performance. Biomedical Materials (Bristol), 2017, 12, 025008.	1.7	27
182	Phase conversion of tricalcium phosphate into Ca-deficient apatite during sintering of hydroxyapatite–tricalcium phosphate biphasic ceramics. Journal of Biomedical Materials Research - Part B Applied Biomaterials, 2008, 84B, 334-339.	1.6	26
183	Improving the strength and biocompatibility of porous titanium scaffolds by creating elongated pores coated with a bioactive, nanoporous TiO2 layer. Materials Letters, 2010, 64, 2526-2529.	1.3	26
184	Acceleration of the healing process of full-thickness wounds using hydrophilic chitosan–silica hybrid sponge in a porcine model. Journal of Biomaterials Applications, 2018, 32, 1011-1023.	1.2	26
185	Hydroxyapatite/poly( <i>É&gt;</i> -caprolactone) double coating on magnesium for enhanced corrosion resistance and coating flexibility. Journal of Biomaterials Applications, 2013, 28, 617-625.	1.2	25
186	Improvement in oxidation resistance of carbon by formation of a protective SiO2 layer on the surface. Journal of the European Ceramic Society, 2001, 21, 2407-2412.	2.8	24
187	Effect of Oxidation on the Roomâ€Temperature Flexural Strength of Reactionâ€Bonded Silicon Carbides. Journal of the American Ceramic Society, 1999, 82, 1601-1604.	1.9	24
188	Fabrication and Characterization of Thin and Dense Electrolyte-Coated Anode Tube Using Thermoplastic Coextrusion. Journal of the American Ceramic Society, 2006, 89, 1713-1716.	1.9	24
189	Enhancement of mechanical properties of grade 4 titanium by equal channel angular pressing with billet encapsulation. Materials Letters, 2014, 114, 144-147.	1.3	24
190	Facile strategy involving low-temperature chemical cross-linking to enhance the physical and biological properties of hyaluronic acid hydrogel. Carbohydrate Polymers, 2018, 202, 545-553.	5.1	24
191	Digital light processing of zirconia prostheses with high strength and translucency for dental applications. Ceramics International, 2020, 46, 28211-28218.	2.3	24
192	Long-lasting and bioactive hyaluronic acid-hydroxyapatite composite hydrogels for injectable dermal fillers: Physical properties and in vivo durability. Journal of Biomaterials Applications, 2016, 31, 464-474.	1.2	23
193	Ta ion implanted nanoridge-platform for enhanced vascular responses. Biomaterials, 2019, 223, 119461.	5.7	23
194	Enhanced endothelial cell activity induced by incorporation of nano-thick tantalum layer in artificial vascular grafts. Applied Surface Science, 2020, 508, 144801.	3.1	23
195	Preparation and Characterization of Sol—Gelâ€Derived Lead Magnesium Niobium Titanate Thin Films with Pure Perovskite Phase and Lead Oxide Cover Coat. Journal of the American Ceramic Society, 2002, 85, 2001-2004.	1.9	22
196	Highly Porous Biphasic Calcium Phosphate ( <scp>BCP</scp> ) Ceramics with Large Interconnected Pores by Freezing Vigorously Foamed <scp>BCP</scp> Suspensions under Reduced Pressure. Journal of the American Ceramic Society, 2011, 94, 4154-4156.	1.9	22
197	Production of highly aligned porous alumina ceramics by extruding frozen alumina/camphene body. Journal of the European Ceramic Society, 2011, 31, 1945-1950.	2.8	22
198	In-vitro blood and vascular compatibility of sirolimus-eluting organic/inorganic hybrid stent coatings. Colloids and Surfaces B: Biointerfaces, 2019, 179, 405-413.	2.5	22

#	Article	IF	CITATIONS
199	Fluorine-ion-releasing injectable alginate nanocomposite hydrogel for enhanced bioactivity and antibacterial property. International Journal of Biological Macromolecules, 2019, 123, 866-877.	3.6	22
200	3D-printed biodegradable composite scaffolds with significantly enhanced mechanical properties via the combination of binder jetting and capillary rise infiltration process. Additive Manufacturing, 2021, 41, 101988.	1.7	22
201	Microstructural Evolution of Gasâ€Pressure‣intered Si <sub>3</sub> N <sub>4</sub> with Yb <sub>2</sub> O <sub>3</sub> as a Sintering Aid. Journal of the American Ceramic Society, 1997, 80, 2737-2740.	1.9	21
202	Production of Aluminum?Zirconium Oxide Hybridized Nanopowder and Its Nanocomposite. Journal of the American Ceramic Society, 2007, 90, 298-302.	1.9	21
203	Synthesis of nanoporous calcium phosphate spheres using poly(acrylic acid) as a structuring unit. Materials Letters, 2009, 63, 1207-1209.	1.3	21
204	Synthesis of poly(ε-caprolactone)/hydroxyapatite nanocomposites using in-situ co-precipitation. Materials Science and Engineering C, 2010, 30, 777-780.	3.8	21
205	Production and characterization of calcium phosphate (CaP) whisker-reinforced poly(Îμ-caprolactone) composites as bone regenerative. Materials Science and Engineering C, 2010, 30, 1280-1284.	3.8	21
206	Production, mechanical properties and in vitro biocompatibility of highly aligned porous poly(Îμ-caprolactone) (PCL)/hydroxyapatite (HA) scaffolds. Journal of Porous Materials, 2013, 20, 701-708.	1.3	21
207	The accelerating effect of chitosan-silica hybrid dressing materials on the early phase of wound healing. , 2017, 105, 1828-1839.		21
208	Novel additive manufacturing of photocurable ceramic slurry containing freezing vehicle as porogen for hierarchical porous structure. Ceramics International, 2019, 45, 21321-21327.	2.3	21
209	Accelerated biodegradation of iron-based implants via tantalum-implanted surface nanostructures. Bioactive Materials, 2022, 9, 239-250.	8.6	21
210	PZN-PZT flextensional actuator by co-extrusion process. Sensors and Actuators A: Physical, 2005, 119, 221-227.	2.0	20
211	Processing and Performance of Hydroxyapatite/Fluorapatite Double Layer Coating on Zirconia by the Powder Slurry Method. Journal of the American Ceramic Society, 2006, 89, 2466-2472.	1.9	20
212	Reaction sintering of lead zinc niobate–lead zirconate titanate ceramics. Journal of the European Ceramic Society, 2006, 26, 111-115.	2.8	20
213	Collagen–silica xerogel nanohybrid membrane for guided bone regeneration. Journal of Biomedical Materials Research - Part A, 2012, 100A, 841-847.	2.1	20
214	Production of highly porous titanium (Ti) scaffolds by vacuum-assisted foaming of titanium hydride (TiH2) suspension. Materials Letters, 2014, 120, 228-231.	1.3	20
215	Effect of HF/HNO3-treatment on the porous structure and cell penetrability of titanium (Ti) scaffold. Materials and Design, 2018, 145, 65-73.	3.3	20
216	Dual-scale porous biphasic calcium phosphate gyroid scaffolds using ceramic suspensions containing polymer microsphere porogen for digital light processing. Ceramics International, 2021, 47, 11285-11293.	2.3	20

#	Article	IF	CITATIONS
217	A combination strategy of functionalized polymer coating with Ta ion implantation for multifunctional and biodegradable vascular stents. Journal of Magnesium and Alloys, 2021, 9, 2194-2206.	5.5	20
218	Strengthening and Prevention of Oxidation of Aluminum Nitride by Formation of a Silica Layer on the Surface. Journal of the American Ceramic Society, 2000, 83, 306-310.	1.9	19
219	Piezoelectric linear motor with unimorph structure by co-extrusion process. Sensors and Actuators A: Physical, 2008, 147, 300-303.	2.0	19
220	Silica-chitosan hybrid coating on Ti for controlled release of growth factors. Journal of Materials Science: Materials in Medicine, 2011, 22, 2757-2764.	1.7	19
221	Biocompatibility of Fluor-Hydroxyapatite Bioceramics. Journal of the American Ceramic Society, 2005, 88, 1309-1311.	1.9	18
222	Enhanced biocompatibility of CoCr implant material by Ti coating and microâ€arc oxidation. Journal of Biomedical Materials Research - Part B Applied Biomaterials, 2009, 90B, 165-170.	1.6	18
223	Porous TiO2 films on Ti implants for controlled release of tetracycline-hydrochloride (TCH). Thin Solid Films, 2011, 519, 8074-8076.	0.8	18
224	Deposition of titanium nitride (TiN) on Co–Cr and their potential application as vascular stent. Applied Surface Science, 2012, 258, 2864-2868.	3.1	18
225	Novel Ceramic/Campheneâ€Based Coâ€Extrusion for Highly Aligned Porous Alumina Ceramic Tubes. Journal of the American Ceramic Society, 2012, 95, 1803-1806.	1.9	18
226	Biomechanical Evaluation of Magnesium-Based Resorbable Metallic Screw System in a Bilateral Sagittal Split Ramus Osteotomy Model Using Three-Dimensional Finite Element Analysis. Journal of Oral and Maxillofacial Surgery, 2014, 72, 402.e1-402.e13.	0.5	18
227	Synthesis and evaluation of bone morphogenetic protein (BMP)-loaded hydroxyapatite microspheres for enhanced bone regeneration. Ceramics International, 2016, 42, 7748-7756.	2.3	18
228	Radiological, histological, and hematological evaluation of hydroxyapatite oated resorbable magnesium alloy screws placed in rabbit tibia. Journal of Biomedical Materials Research - Part B Applied Biomaterials, 2017, 105, 1636-1644.	1.6	18
229	In vitro and in vivo evaluation of polylactic acid-based composite with tricalcium phosphate microsphere for enhanced biodegradability and osseointegration. Journal of Biomaterials Applications, 2018, 32, 1360-1370.	1.2	18
230	Chitosan-Based Dressing Materials for Problematic Wound Management. Advances in Experimental Medicine and Biology, 2018, 1077, 527-537.	0.8	18
231	Improvement in oxidation resistance of TiB <sub>2</sub> by formation of protective SiO <sub>2</sub> layer on surface. Journal of Materials Research, 2001, 16, 132-137.	1.2	17
232	Hydroxyapatite-based composite for dental implants: Anin vivo removal torque experiment. Journal of Biomedical Materials Research Part B, 2002, 63, 714-721.	3.0	17
233	Improved Lowâ€Temperature Environmental Degradation of Yttriaâ€Stabilized Tetragonal Zirconia Polycrystals by Surface Encapsulation. Journal of the American Ceramic Society, 1999, 82, 1456-1458.	1.9	17
234	Novel rapid direct deposition of ceramic paste for porous biphasic calcium phosphate (BCP) scaffolds with tightly controlled 3-D macrochannels. Ceramics International, 2014, 40, 11079-11084.	2.3	17

#	Article	IF	CITATIONS
235	Digital Light Processing of Freeze-cast Ceramic Layers for Macroporous Calcium Phosphate Scaffolds with Tailored Microporous Frameworks. Materials, 2019, 12, 2893.	1.3	17
236	Improving mechanical properties of porous calcium phosphate scaffolds by constructing elongated gyroid structures using digital light processing. Ceramics International, 2021, 47, 3252-3258.	2.3	17
237	Microstructure and Fracture Toughness of Hot-Pressed Silicon Carbide Reinforced with Silicon Carbide Whisker. Journal of the American Ceramic Society, 1994, 77, 3270-3272.	1.9	16
238	Multilayer Actuator Composed of PZN-PZT and PZN-PZT/Ag Fabricated by Co-Extrusion Process. Journal of the American Ceramic Society, 2005, 88, 1625-1627.	1.9	16
239	On the feasibility of phosphate glass and hydroxyapatite engineered coating on titanium. Journal of Biomedical Materials Research - Part A, 2005, 75A, 656-667.	2.1	16
240	Microstructural evolution and piezoelectric properties of thick Pb(Zr,Ti)O3 films deposited by multi-sputtering method: Part I. Microstructural evolution. Journal of Materials Research, 2007, 22, 1367-1372.	1.2	16
241	Thick Pb(Zr,Ti)O3 film without substrate. Applied Physics Letters, 2007, 91, .	1.5	16
242	Effect of excess PbO on microstructure and orientation of PZT(60/40) films. Journal of Electroceramics, 2010, 25, 20-25.	0.8	16
243	Hollow porous poly(ε-caprolactone) microspheres by emulsion solvent extraction. Materials Letters, 2012, 72, 157-159.	1.3	16
244	Large-scale nanopatterning of metal surfaces by target-ion induced plasma sputtering (TIPS). RSC Advances, 2016, 6, 23702-23708.	1.7	16
245	Hyaluronic acidâ€hydroxyapatite nanocomposite hydrogels for enhanced biophysical and biological performance in a dermal matrix. Journal of Biomedical Materials Research - Part A, 2017, 105, 3315-3325.	2.1	16
246	Enhancement of osseointegration by direct coating of rhBMP-2 on target-ion induced plasma sputtering treated SLA surface for dental application. Journal of Biomaterials Applications, 2017, 31, 807-818.	1.2	16
247	Biocompatibility and Biocorrosion of Hydroxyapatite-Coated Magnesium Plate: Animal Experiment. Materials, 2017, 10, 1149.	1.3	16
248	Characterization of Titanium Surface Modification Strategies for Osseointegration Enhancement. Metals, 2021, 11, 618.	1.0	16
249	Oxidation Behavior and Effect of Oxidation on Strength of Si3N4/SiC Nanocomposites. Journal of Materials Research, 2000, 15, 1478-1482.	1.2	15
250	Orientation control of sol-gel-derived lead zirconate titanate film by addition of polyvinylpyrrolidone. Journal of Materials Research, 2005, 20, 882-888.	1.2	15
251	Deposition of TiN films on Co–Cr for improving mechanical properties and biocompatibility using reactive DC sputtering. Journal of Materials Science: Materials in Medicine, 2011, 22, 2231-2237.	1.7	15
252	Creation of nanoporous tantalum (Ta)-incorporated titanium (Ti) surface onto Ti implants by sputtering of Ta in Ar under extremely high negative substrate biases. Journal of Materials Chemistry, 2012, 22, 24798.	6.7	15

#	Article	IF	CITATIONS
253	Novel self-assembly-induced 3D plotting for macro/nano-porous collagen scaffolds comprised of nanofibrous collagen filaments. Materials Letters, 2015, 143, 265-268.	1.3	15
254	Growth of highly (100) oriented lead zirconate titanate films on silicon and glass substrates using lanthanum nitrate as a buffer layer. Applied Physics Letters, 2004, 85, 4621-4623.	1.5	14
255	Improving hardness of biomedical Co–Cr by deposition of dense and uniform TiN films using negative substrate bias during reactive sputtering. Materials Letters, 2011, 65, 1707-1709.	1.3	14
256	Production of porous poly(Îμ-caprolactone)/silica hybrid membranes with patterned surface pores. Materials Letters, 2011, 65, 1903-1906.	1.3	14
257	Synthesis of nanofibrous gelatin/silica bioglass composite microspheres using emulsion coupled with thermally induced phase separation. Materials Science and Engineering C, 2016, 62, 678-685.	3.8	14
258	Ultrafine-grained porous titanium and porous titanium/magnesium composites fabricated by space holder-enabled severe plastic deformation. Materials Science and Engineering C, 2016, 59, 754-765.	3.8	14
259	Coextrusion-Based 3D Plotting of Ceramic Pastes for Porous Calcium Phosphate Scaffolds Comprised of Hollow Filaments. Materials, 2018, 11, 911.	1.3	14
260	Stable sol–gel hydroxyapatite coating on zirconia dental implant for improved osseointegration. Journal of Materials Science: Materials in Medicine, 2021, 32, 81.	1.7	14
261	Functionally assembled metal platform as lego-like module system for enhanced mechanical tunability and biomolecules delivery. Materials and Design, 2021, 207, 109840.	3.3	14
262	Microstructural evolution and mechanical properties of Si3N4–SiC (nanoparticle)–Si3N4 (whisker) composites. Journal of Materials Research, 2000, 15, 364-368.	1.2	13
263	Effects of lanthanum nitrate buffer layer on the orientation and piezoelectric property of Pb(Zr,Ti)O3 thick film. Journal of Materials Research, 2004, 19, 3671-3678.	1.2	13
264	Strengthening of Alumina by Formation of a Mullite/Glass Layer on the Surface. Journal of the American Ceramic Society, 1997, 80, 1877-1880.	1.9	13
265	Mechanical Properties of Si <sub>3</sub> N <sub>4</sub> â€SiC Threeâ€Layer Composite Materials. Journal of the American Ceramic Society, 1998, 81, 2725-2728.	1.9	13
266	Piezoelectric Multilayer Ceramic/Polymer Composite Transducer with 2–2 Connectivity. Journal of the American Ceramic Society, 2006, 89, 2509-2513.	1.9	13
267	Production of Hydroxyapatite/Bioactive Glass Biomedical Composites by the Hot-Pressing Technique. Journal of the American Ceramic Society, 2006, 89, 3593-3596.	1.9	13
268	Microstructural evolution and piezoelectric properties of thick Pb(Zr,Ti)O3 films deposited by the multi-sputtering method: Part II. Piezoelectric properties. Journal of Materials Research, 2007, 22, 1373-1377.	1.2	13
269	Ti scaffolds with tailored porosities and mechanical properties using porous polymer templates. Materials and Design, 2016, 101, 323-331.	3.3	13
270	Dual rosslinking of Hyaluronic Acid–Calcium Phosphate Nanocomposite Hydrogels for Enhanced Mechanical Properties and Biological Performance. Macromolecular Materials and Engineering, 2017, 302, 1700160.	1.7	13

#	Article	IF	CITATIONS
271	Bifunctional poly (l-lactic acid)/hydrophobic silica nanocomposite layer coated on magnesium stents for enhancing corrosion resistance and endothelial cell responses. Materials Science and Engineering C, 2021, 127, 112239.	3.8	13
272	Microstructural evolution and mechanical properties of gas-pressure-sintered Si <sub>3</sub> N <sub>4</sub> with Yb <sub>2</sub> O <sub>3</sub> as a sintering aid. Journal of Materials Research, 1999, 14, 1904-1909.	1.2	12
273	Reinforcement of a Reticulated Porous Ceramic by a Novel Infiltration Technique. Journal of the American Ceramic Society, 2006, 89, 060427083300080-???.	1.9	12
274	The impact of immobilization of BMPâ€⊋ on PDO membrane for bone regeneration. Journal of Biomedical Materials Research - Part A, 2012, 100A, 1488-1493.	2.1	12
275	Ultrafast Singleâ€Band Upconversion Luminescence in a Liquidâ€Quenched Amorphous Matrix. Advanced Materials, 2018, 30, 1800008.	11.1	12
276	Piezoelectric ultrasonic motor by co-extrusion process. Sensors and Actuators A: Physical, 2005, 121, 515-519.	2.0	11
277	Fabrication and Characterization of Dual-Channeled Zirconia Ceramic Scaffold. Journal of the American Ceramic Society, 2006, 89, 2021-2026.	1.9	11
278	Effects of Excess PbO and Zr/Ti Ratio on Microstructure and Electrical Properties of PZT Films. Journal of the American Ceramic Society, 2008, 91, 2923-2927.	1.9	11
279	Electrodeposition of biodegradable sol–gel derived silica onto nanoporous TiO2 surface formed on Ti substrate. Materials Letters, 2011, 65, 1519-1521.	1.3	11
280	Use of Glycerol as a Cryoprotectant in Vacuumâ€Assisted Foaming of Ceramic Suspension Technique for Improving Compressive Strength of Porous Biphasic Calcium Phosphate Ceramics. Journal of the American Ceramic Society, 2012, 95, 3360-3362.	1.9	11
281	Nonsolvent induced phase separation (NIPS)-based 3D plotting for 3-dimensionally macrochanneled poly(ε-caprolactone) scaffolds with highly porous frameworks. Materials Letters, 2014, 122, 348-351.	1.3	11
282	Biomimetic Coating of Hydroxyapatite on Glycerol Phosphate-Conjugated Polyurethane via Mineralization. ACS Omega, 2017, 2, 981-987.	1.6	11
283	Incorporation of Calcium Sulfate Dihydrate into Hydroxyapatite Microspheres To Improve the Release of Bone Morphogenetic Protein-2 and Accelerate Bone Regeneration. ACS Biomaterials Science and Engineering, 2018, 4, 846-856.	2.6	11
284	Bioactive and mechanically stable hydroxyapatite patterning for rapid endothelialization of artificial vascular graft. Materials Science and Engineering C, 2020, 106, 110287.	3.8	11
285	Nano-Topographical Control of Ti-Nb-Zr Alloy Surfaces for Enhanced Osteoblastic Response. Nanomaterials, 2021, 11, 1507.	1.9	11
286	Random exchange-type electro-optic behavior of Pb0.865La0.09(Zr0.65Ti0.35)O3 relaxor ferroelectrics. Applied Physics Letters, 2002, 81, 706-708.	1.5	10
287	Piezoelectric Fibers with Uniform Internal Electrode by Co-Extrusion Process. Journal of the American Ceramic Society, 2006, 89, 1333-1336.	1.9	10
288	Improvement in Biocompatibility of Fluoridated Apatite with Addition of Resorbable Glass. Journal of the American Ceramic Society, 2006, 89, 1748-1751.	1.9	10

#	Article	IF	CITATIONS
289	Fabrication of ultrahigh porosity ceramics with biaxial pore channels. Materials Letters, 2006, 60, 878-882.	1.3	10
290	Transverse 1-3 piezoelectric ceramic/polymer composite with multi-layered PZT ceramic blocks. Sensors and Actuators A: Physical, 2007, 134, 480-485.	2.0	10
291	Production and evaluation of porous titanium scaffolds with 3-dimensional periodic macrochannels coated with microporous TiO2 layer. Materials Chemistry and Physics, 2012, 135, 897-902.	2.0	10
292	Novel Self-Assembly-Induced Gelation for Nanofibrous Collagen/Hydroxyapatite Composite Microspheres. Materials, 2017, 10, 1110.	1.3	10
293	Design and Production of Continuously Gradient Macro/Microporous Calcium Phosphate (CaP) Scaffolds Using Ceramic/Camphene-Based 3D Extrusion. Materials, 2017, 10, 719.	1.3	10
294	Enhanced Bioactivity of Micropatterned Hydroxyapatite Embedded Poly(L-lactic) Acid for a Load-Bearing Implant. Polymers, 2020, 12, 2390.	2.0	10
295	Macrochanneled Tetragonal Zirconia Polycrystals Coated by a Calcium Phosphate Layer. Journal of the American Ceramic Society, 2003, 86, 2027-2030.	1.9	9
296	Birefringence study of the freezing mechanism of lanthanum-modified lead zirconate titanate relaxor ferroelectrics. Journal of Applied Physics, 2003, 93, 1176-1179.	1.1	9
297	Thermoplastic Green Machining for the Fabrication of a Piezoelectric Ceramic/Polymer Composite with 2-2 Connectivity. Journal of the American Ceramic Society, 2005, 88, 1060-1063.	1.9	9
298	Helical-shaped piezoelectric motor using thermoplastic co-extrusion process. Sensors and Actuators A: Physical, 2010, 158, 294-299.	2.0	9
299	Rapid direct deposition of TiH2 paste for porous Ti scaffolds with tailored porous structures and mechanical properties. Materials Chemistry and Physics, 2016, 176, 104-109.	2.0	9
300	Tantalum – Poly (L-lactic acid) nerve conduit for peripheral nerve regeneration. Neuroscience Letters, 2020, 731, 135049.	1.0	9
301	Novel camphene/photopolymer solution as pore-forming agent for photocuring-assisted additive manufacturing of porous ceramics. Journal of the European Ceramic Society, 2021, 41, 655-662.	2.8	9
302	Domain Morphology and Field-Induced Phase Transition in 'Two Phase Zone' of PZN-Based Ferroelectrics. Ferroelectrics, 2002, 269, 33-38.	0.3	8
303	Fabrication and compressive strength of macrochannelled tetragonal zirconia polycrystals with calcium phosphate coating layer. Journal of Materials Research, 2003, 18, 2009-2012.	1.2	8
304	Effect of residual stress on piezoelectric property of Pb(Zr,Ti)O3 films fabricated by sol-gel process. Journal of Sol-Gel Science and Technology, 2007, 42, 305-308.	1.1	8
305	Synthesis and Characterization of Drug-Loaded Poly( <mml:math) 0.784314="" 1="" 10="" 50<="" etqq1="" overlock="" rgbt="" td="" tf="" tj=""><td>112 Td (xr 1.5</td><td>nlns:mml="h 8</td></mml:math)>	112 Td (xr 1.5	nlns:mml="h 8
	Nanofibrous Scaffolds. Journal of Nanomaterials. 2013, 2013, 1-12.		
306	Fabrication of Mechanically Tunable and Bioactive Metal Scaffolds for Biomedical Applications. Journal of Visualized Experiments, 2015, , e53279.	0.2	8

#	Article	IF	CITATIONS
307	Novel Threeâ€Dimensional Extrusion of Multilayered Ceramic/Camphene Mixture for Gradient Porous Ceramics. Journal of the American Ceramic Society, 2016, 99, 395-398.	1.9	8
308	UV curing–assisted 3D plotting of core-shelled feedrod for macroporous hydroxyapatite scaffolds comprised of microporous hollow filaments. Journal of the European Ceramic Society, 2021, 41, 6729-6737.	2.8	8
309	Customizable design of multiple-biomolecule delivery platform for enhanced osteogenic responses via â€~tailored assembly system'. Bio-Design and Manufacturing, 2022, 5, 451-464.	3.9	8
310	Evaluation of Whisker Alignment in Axisymmetric SiCw-Reinforced Al2O3 Composite Material. Journal of the American Ceramic Society, 1994, 77, 2828-2832.	1.9	7
311	Electrooptic properties of highly oriented Pb(Zr,Ti)O3 film grown on glass substrate using lanthanum nitrate as a buffer layer. Journal of Materials Research, 2004, 19, 3152-3156.	1.2	7
312	Mechanical Properties of Three‣ayered Monolithic Silicon Nitride–Fibrous Silicon Nitride/Boron Nitride Monolith. Journal of the American Ceramic Society, 2002, 85, 2840-2842.	1.9	7
313	Effect of Electrode Configuration on Phase Retardation of PLZT Films Grown on Glass Substrate. Journal of the American Ceramic Society, 2004, 87, 950-952.	1.9	7
314	Mechanical and Biological Performance of Calcium Phosphate Coatings on Porous Bone Scaffold. Journal of the American Ceramic Society, 2004, 87, 2135-2138.	1.9	7
315	Sol-Gel Preparation of Thick PZN-PZT Film Using a Diol-Based Solution Containing Polyvinylpyrrolidone for Piezoelectric Applications. Journal of the American Ceramic Society, 2005, 88, 3049-3054.	1.9	7
316	Effects of Thickness on Piezoelectric Properties of Highly Oriented Lead Zirconate Titanate Films. Journal of the American Ceramic Society, 2006, 89, 060427083300082-???.	1.9	7
317	Multilayer bender-type PZT-PZN actuator by co-extrusion process. Journal of the European Ceramic Society, 2006, 26, 2345-2348.	2.8	7
318	Production of porous Calcium Phosphate (CaP) ceramics with aligned pores using ceramic/camphene-based co-extrusion. Biomaterials Research, 2015, 19, 16.	3.2	7
319	Effect of lithium content on spinel phase evolution in the composite material LixNi0.25Co0.10Mn0.65O(3.4+x)/2 (0.8≤â‰⊉.6) for Li-ion batteries. Solid State Ionics, 2016, 293, 77-84.	1.3	7
320	Strategy for Preparing Mechanically Strong Hyaluronic Acid–Silica Nanohybrid Hydrogels via In Situ Sol–Gel Process. Macromolecular Materials and Engineering, 2018, 303, 1800213.	1.7	7
321	PLLA Membrane with Embedded Hydroxyapatite Patterns for Improved Bioactivity and Efficient Delivery of Growth Factor. Macromolecular Bioscience, 2020, 20, 2000136.	2.1	7
322	Effect of Oxidation on Mechanical Properties of Fibrous Monolith Si <sub>3</sub> N <sub>4</sub> /BN at Elevated Temperatures in Air. Journal of the American Ceramic Society, 2002, 85, 3123-3125.	1.9	6
323	Râ€Curve Behavior of Silicon Nitride Ceramic Reinforced with Silicon Carbide Platelets. Journal of the American Ceramic Society, 1998, 81, 2191-2193.	1.9	6
324	Spiral-shaped piezoelectric actuator fabricated using thermoplastic co-extrusion process. Sensors and Actuators A: Physical, 2008, 148, 245-249.	2.0	6

#	Article	IF	CITATIONS
325	3D Plotting using Camphene as Pore-regulating Agent to Produce Hierarchical Macro/micro-porous Poly(ε-caprolactone)/calcium phosphate Composite Scaffolds. Materials, 2019, 12, 2650.	1.3	6
326	Recombinant osteopontin fragment coating on hydroxyapatite for enhanced osteoblast-like cell responses. Journal of Materials Science, 2005, 40, 2891-2895.	1.7	5
327	Thick Pb(Zr,Ti)O3 films fabricated by inducing residual compressive stress during the annealing process. Journal of Materials Research, 2005, 20, 2898-2901.	1.2	5
328	Windmill-type ultrasonic micromotor fabricated by thermoplastic green machining process. Sensors and Actuators A: Physical, 2007, 134, 519-524.	2.0	5
329	Fabrication of highly porous titanium (Ti) scaffolds with two interlaced periodic pores. Materials Letters, 2009, 63, 1341-1343.	1.3	5
330	Fabrication of porous calcium phosphate cements using gelatin as porogen. Journal of the Ceramic Society of Japan, 2010, 118, 34-36.	0.5	5
331	Calcium phosphate ceramics with continuously gradient macrochannels using three-dimensional extrusion of bilayered ceramic-camphene mixture/pure camphene feedrod. Ceramics International, 2016, 42, 15603-15609.	2.3	5
332	Multilayered Polyurethane–Hydroxyapatite Composite for Meniscus Replacements. Macromolecular Materials and Engineering, 2019, 304, 1800352.	1.7	5
333	Novel poly(ε-caprolactone) scaffolds comprised of tailored core/shell-structured filaments using 3D plotting technique. Materials Letters, 2020, 269, 127659.	1.3	5
334	Effect of Manganese Ion Diffusion on the Microstructural Evolution of Lead Lanthanum Zirconate Titanate Ceramic. Journal of the American Ceramic Society, 2002, 85, 733-735.	1.9	4
335	Piezoelectric properties of lead-free (Na0.5Bi0.5)TiO3–(Na0.5K0.5)NbO3–BaTiO3 ceramics. Journal of Materials Research, 2008, 23, 115-120.	1.2	4
336	Identification and characterization of a novel heparinâ€binding peptide for promoting osteoblast adhesion and proliferation by screening an <i>Escherichia coli</i> cell surface display peptide library. Journal of Peptide Science, 2009, 15, 43-47.	0.8	4
337	Strength and Magnetic Properties of a Laminated Composite of Magnetic Metal Foil and Zirconia. Journal of the American Ceramic Society, 2004, 82, 1349-1351.	1.9	3
338	Co-Firing of Spatially Varying Dielectric Ca-Mg-Silicate and Bi-Ba-Nd-Titanate Composite. Journal of the American Ceramic Society, 2005, 88, 2690-2695.	1.9	3
339	Ferroelectric and piezoelectric properties of highly oriented Pb(Zr,Ti)O3 film grown on Pt/Ti/SiO2/Si substrate using conductive lanthanum nickel nitrate buffer layer. Journal of Materials Research, 2005, 20, 726-733.	1.2	3
340	Electrical properties of highly oriented Pb(Mg1/3Nb2/3)O3–Pb(Zr,Ti)O3 thin films fabricated by the sol-gel method. Journal of Materials Research, 2006, 21, 1532-1536.	1.2	3
341	Zirconia-Polyurethane Aneurysm Clip. World Neurosurgery, 2018, 115, 14-23.	0.7	3
342	Enhanced biolubrication on biomedical devices using hyaluronic acid-silica nanohybrid hydrogels. Colloids and Surfaces B: Biointerfaces, 2019, 184, 110503.	2.5	3

#	Article	IF	CITATIONS
343	Ceramic-Ceramic Actuator Composed of Two Piezoelectric Layers with Opposite Poling Directions. Journal of the American Ceramic Society, 2005, 88, 997-999.	1.9	2
344	Fluoride coatings on orthodontic wire for controlled release of fluorine ion. Journal of Biomedical Materials Research - Part B Applied Biomaterials, 2005, 75B, 200-204.	1.6	2
345	Improved Biocompatibility of Intra-Arterial Poly-L-Lactic Acid Stent by Tantalum Ion Implantation : 3-Month Results in a Swine Model. Journal of Korean Neurosurgical Society, 2021, 64, 853-863.	0.5	2
346	Effects of Heat Treatment in a Wet Hydrogen Atmosphere on the Reliability of Sintered alpha-Silicon Carbide. Journal of the American Ceramic Society, 1995, 78, 1708-1710.	1.9	1
347	Electrostrictive properties and polarization mechanisms of Pb(Zn1/3Nb2/3)O3based ceramics. Ferroelectrics, 2001, 261, 89-94.	0.3	1
348	Improvement in crystallinity of apatite coating on titanium with the insertion of CaF2 buffer layer. Journal of Materials Science: Materials in Medicine, 2008, 19, 1905-1911.	1.7	1
349	Preparation of Hyaluronicâ€Acidâ€Based Microspherical Particles with Tunable Morphology Using a Spray Method on a Superhydrophobic Surface. Macromolecular Materials and Engineering, 2019, 304, 1900100.	1.7	1
350	Use of thioglycerol on porous polyurethane as an effective theranostic capping agent for bone tissue engineering. Journal of Biomaterials Applications, 2019, 33, 955-966.	1.2	1
351	Domain Morphology and Field-Induced Phase Transition in 'Two Phase Zone' of PZN-Based Ferroelectrics. , 0, .		1
352	Effect of Si3N4-whisker addition on microstructural development and fracture toughness of hot-isostatically pressed Si3N4. Journal of Materials Science Letters, 1994, 13, 1249-1251.	0.5	0
353	Electric field dependence of the dielectric properties of Pb(Zn1/3Nb2/3)O3-BaTiO3-PbTiO3ceramics. Ferroelectrics, 2001, 262, 155-160.	0.3	0
354	Improvement of oxidation resistance of Si3N4 by heat treatment in a wet H2 atmosphere. Journal of Materials Research, 2002, 17, 2321-2326.	1.2	0
355	Electro-Optic Characteristics of PLZT 9/65/35 Relaxor Ferroelectrics. Ferroelectrics, 2002, 273, 173-178.	0.3	0
356	Deposition of Highly (100) Oriented PZT Film Using Lanthanum Nitrate/Nickel Acetate Buffer Layer. Materials Research Society Symposia Proceedings, 2005, 902, 1.	0.1	0
357	Biological Activities of HA-coated Zirconia. The Journal of the Korean Academy of Periodontology, 2003, 33, 1.	0.1	0